JOURNAL OF PETROLOGY | VOLUME 36 | NUMBER 6 | PAGES 1633–1646 | 1995

JACQUELINE EABY DIXON*AND EDWARD M. STOLPER
DIVISION OF GEOLOGICAL AND PLANETARY SCIENCES, CALIFORNIA INSTITUTE OF TECHNOLOGY, PASADENA, CA 91125, USA

An Experimental Study of Water and Carbon Dioxide Solubilities in Mid-Ocean Ridge Basaltic Liquids. Part II: Applications to Degassing

Degassing processes in basaltic magmas rich in both water and carbon dioxide can be modeled using the solubilities of the end-member systems and the assumption of Henry's law. Suites of vapor-saturated basaltic melts having a range of initial CO_2/H_2O ratios and erupted over a narrow depth interval will define negatively sloped arrays on an H_2O vs CO_2 plot. It is important that all of the major volatile species be considered simultaneously when interpreting trends in dissolved volatile species concentrations in magmas.

Based on measured concentrations of water and carbon dioxide in basaltic glasses, the composition of the vapor phase at 1200°C that could coexist with a basaltic melt and the pressure at which it would be vapor saturated can be calculated. The range in vapor compositions in equilibrium with submarine basalts reflects the range in water contents in the melts characteristic of each environment. The ranges in the molar proportion of CO_2 in vapor phases ($X^v_{CO_2}$) calculated to be in equilibrium with submarine tholeiitic glasses are 0·93–1·00 for mid-ocean ridge basalts (MORB), 0·60–0·99 for glasses from Kilauea [representative of ocean island basalts (OIB)] and 0–0·94 for glasses from back-arc basins (BABB). MORB glasses from spreading centers ranging from slow (e.g. the Mid-Atlantic Ridge) to fast (e.g. East Pacific Rise, 9–13°N) are commonly supersaturated with respect to CO_2-rich vapor, resulting from magma ascent rates so rapid that magmas erupt on the sea-floor without having been fully degassed by bubble nucleation and growth during ascent. In contrast to the MORB glasses, volatile contents in submarine glasses from Kilauea are consistent with having been in equilibrium with a vapor phase containing 60–100 mol % CO_2 at the pressure of eruption, reflecting differences in average magma transport rates during eruptions at mid-ocean ridges and hot-spot volcanoes.

Degassing during decompression of tholeiitic basaltic magma is characterized by strong partitioning of CO_2 into the vapor phase. During open system degassing, CO_2 is rapidly removed from the melt with negligible loss of water, until a pressure is reached at which the melt is in equilibrium with nearly pure water vapor. From this pressure downward, the water content of the melt follows the water solubility curve. During closed system degassing, water and CO_2 contents in vapor-saturated basaltic magmas will depend strongly on the vapor composition as determined by the initial volatile concentrations. Deviation from open system behavior, toward lower dissolved H_2O and CO_2 saturation concentrations at a given pressure, will be greatest in melts having high total volatile concentrations and high CO_2:H_2O ratios. Closed system degassing of basaltic melts having the low initial H_2O and CO_2 contents typical of MORB and OIB, however, are similar to the open system case.

KEY WORDS: *mid-ocean ridge basalts; water and carbon dioxide solubility; degassing*

INTRODUCTION

Most, if not all, submarine and subaerial magmas contain vapor-filled bubbles on eruption and emplacement. There is growing interest in the role of volatiles in igneous processes, including the timing of volatile exsolution and bubble growth and its relation to the bulk physical properties of melts and eruption dynamics (Moore *et al.*, 1977; Moore, 1979; Vergniolle & Jaupart, 1986, 1990; Jaupart & Vergniolle, 1988, 1989; Tait *et al.*, 1989; Bottinga & Javoy, 1990*a*,*b*; Mangan *et al.*, 1993) and the estimation of degassing rates of CO_2, H_2O, F, Cl and

*Corresponding author. Present address: Rosenstiel School of Marine and Atmospheric Science, Division of Marine Geology and Geophysics, University of Miami, Miami, FL 33149-1098, USA

S from volcanoes on scales ranging from the evolution of an individual volcano (e.g. Jagger, 1940; Le Guern *et al.*, 1979; Gerlach, 1986, 1989; Gerlach & Graeber, 1985; Gerlach & Casadevall, 1986; Kodosky *et al.*, 1991; Symonds *et al.*, 1992; Brantley *et al.*, 1993) to global fluxes (e.g. Anderson, 1974; Javoy *et al.*, 1982; Pineau & Javoy, 1983; Devine *et al.*, 1984; Des Marais, 1985; Marty & Jambon, 1987; Stoiber *et al.*, 1987; Gerlach, 1989; Palais & Sigurdsson, 1989; Williams *et al.*, 1992; Jambon, 1994). Also, the effects of eruptive degassing must be understood before volatile contents measured in volcanic glasses can be used to investigate primary variations in volatile contents of magmas and their source regions (e.g. Moore, 1970; Delaney *et al.*, 1978; Schilling *et al.*, 1980, 1983; Byers *et al.*, 1983, 1984, 1986; Michael & Chase, 1987; Dixon *et al.*, 1988; Michael, 1988; Michael & Schilling, 1989; Stolper & Newman, 1994).

The solubilities of H_2O and CO_2 and the nature of their mixing behavior in basaltic liquid at 1200°C and pressures relevant to seafloor eruption have been recently determined (Dixon *et al.*, 1995—Part I, this issue). One application of these experimental results is quantification of the behavior of volatiles during degassing. In this paper we present a method for determining the pressure of equilibration between vapor and melt and the composition of a vapor phase that could coexist with a given basaltic melt. We also present new forward degassing models that can be used to predict melt and vapor compositions and vesicularity as a function of pressure and pre-eruptive volatile contents of basaltic magmas.

VOLATILE CONTENTS OF CO_2–H_2O-VAPOR-SATURATED BASALTIC MELTS

Our results (Dixon *et al.*, 1995) can be used to determine the total pressure at which a basaltic liquid with given concentrations of CO_2 and H_2O would be vapor saturated and the composition (i.e. CO_2:H_2O ratio) of vapor coexisting with such a liquid at equilibrium. This is a valuable tool for determining the pressures of vapor–melt equilibration based on measured CO_2 and H_2O concentrations of volcanic glasses; in cases where melt was never vapor saturated, this allows determination of minimum pressures.

If the vapor contains only CO_2 and H_2O, and assuming it mixes ideally (i.e. the Lewis–Randall rule: $f_i = X_i^v f_i^o$, see the Appendix; also, see the Appendix for definitions of terms), the following condition must be satisfied for vapor saturation:

$$\frac{a^m_{H_2O}}{a^{o,m}_{H_2O}} + \frac{a^m_{CO_3^{2-}}}{a^{o,m}_{CO_3^{2-}}} = 1 \qquad (1)$$

where a_i^m is the activity of water or carbonate in the melt and $a_i^{o,m}$ is the corresponding activity in melt in equilibrium with pure water or carbon dioxide. Given the Lewis–Randall rule, it can be shown that the mole fractions of H_2O and CO_2 in the vapor can be determined using $a^m_{H_2O}/a^{o,m}_{H_2O} = X^v_{H_2O}$ and $a^m_{CO_3^{2-}}/a^{o,m}_{CO_3^{2-}} = X^v_{CO_2}$. We adopt the Henrian approximations described by Dixon *et al.* (1995) for both water and carbonate activities, so the activities in equation (1) are just the mole fractions of molecular water and carbonate in the melt. Equation (1) thus reduces to

$$\frac{X^m_{H_2O,\,mol}}{X^{o,m}_{H_2O,\,mol}} + \frac{X^m_{CO_3^{2-}}}{X^{o,m}_{CO_3^{2-}}} = 1. \qquad (2)$$

At constant P and T, the denominators in equation (2) (i.e. the amounts of molecular water and carbon dioxide dissolved in melts coexisting with pure water vapor or carbon dioxide vapor) are constants (i.e. independent of vapor composition) and can be calculated from the following equations [equations (2) and (6) of Dixon *et al.* (1995)]:

$$X^{o,m}_{H_2O,\,mol} = X^{o,m}_{H_2O,\,mol}(P_0, T_0)\frac{f^o_{H_2O}(P, T_0)}{f^o_{H_2O}(P_0, T_0)} \exp\left\{\frac{(-V^{o,m}_{H_2O})(P - P_0)}{RT_0}\right\} \qquad (3)$$

and

$$X^{o,m}_{CO_3^{2-}}(P, T_0) = X^{o,m}_{CO_3^{2-}}(P_0 T_0)\frac{f^o_{CO_2}(P, T_0)}{f^o_{CO_2}(P_0, T_0)} \exp\left\{\frac{(-\Delta V_r^{o,m})(P - P_0)}{RT_0}\right\} \qquad (4)$$

where P is in bars and $P_0 = 1$ bar, $f^o_{H_2O}(P_0, T_0)$ and $f^o_{CO_2}(P_0, T_0) = 1$ bar, T is in K and $T_0 = 1473{\cdot}15$ K, $X^{o,m}_{H_2O,\,mol}(P_0, T_0) = 3{\cdot}28 \times 10^{-5}$, $X^{o,m}_{CO_3^{2-}}(P_0, T_0) = 3{\cdot}8 \times 10^{-7}$, $V^{o,m}_{H_2O} = 12$ cm^3/mol, $\Delta V_r^{o,m} = 23$ cm^3/mol and $R = 83{\cdot}15$ cm^{3}bar/mol-K. Thus, at a constant P and T, equation (2) describes a linear relationship between $X^m_{CO_3^{2-}}$ and $X^m_{H_2O,\,mol}$ as a function of vapor composition in vapor-saturated melts. However, as shown in Fig. 1, the relationship between total dissolved water and dissolved carbonate in vapor-saturated melts at a constant total pressure (isobar)

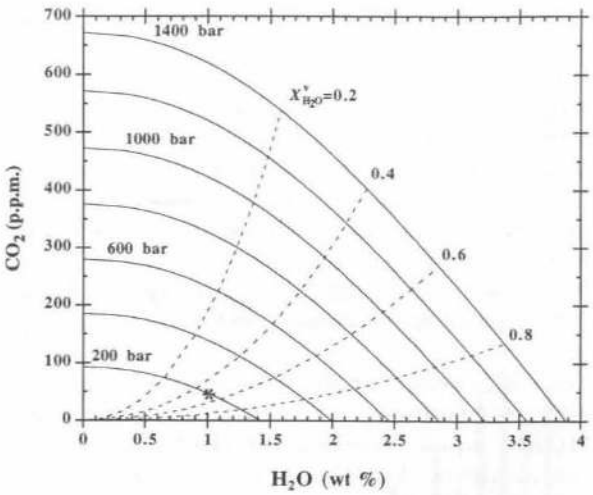

Fig. 1. Inverse correlation between CO_2 and H_2O in vapor-saturated basaltic liquid at constant pressure and 1200°C. Continuous curves are curves of constant pressure (isobars). Dashed curves represent curves for constant vapor composition (isopleths). Curves are calculated using equation (2) combined with a regular solution model for water speciation to calculate total water from molecular water concentrations. This figure can be used to determine the pressure and the composition of the vapor phase in equilibrium with basaltic liquid at vapor saturation. For example, a melt containing 1·0 wt % H_2O and 46 p.p.m. CO_2 (shown as a star in the figure) will be saturated at a pressure of 200 bar (2 km water depth) with a vapor phase having $X^v_{H_2O} = 0{\cdot}5$.

is non-linear because of the non-linear relationship between the concentration of molecular water and total water in basalts [fig. 3a of Dixon *et al.* (1995)]. Similarly, the contours of constant vapor composition (dashed in Fig. 1) are also non-linear. CO_2 is strongly partitioned into the vapor under the conditions of Fig. 1. It can be shown that the ratio $(X^v_{CO_2}/X^v_{H_2O}/X^m_{CO_3^{2-}}/X^m_{H_2O,\,mol})$ is a constant at constant P and T given the assumption of the Lewis–Randall rule. At the low pressures of Fig. 1, this ratio is also only weakly dependent on total pressure, decreasing from 86 at 1 bar to 76 at 1000 bar.

Figure 1 can be used to determine graphically the pressure at which a basaltic liquid with known concentrations of water and carbon dioxide would be vapor saturated at 1200°C and the composition of the vapor phase with which it would be saturated under these conditions. Liquid compositions in vapor-saturated magmas erupted over a narrow depth interval will fall on a single isobar in Fig. 1. We thus expect that analyses of quenched, vesicular glasses spanning a range of CO_2:H_2O ratios and erupted at the same water depth will define negatively sloped arrays on an H_2O vs CO_2 plot, corresponding to the isobar at the pressure of their eruption (provided the melt and vapor are in equilibrium and the vapor is nearly pure H_2O–CO_2). This relationship has only been observed so far in submarine glasses from the Mariana trough (Newman, 1989, 1990; Stolper & Newman, 1994) and the Lau Basin (Newman, 1990), but it is likely to be a general phenomenon. In the case of primitive Mariana trough glasses, the wide range of CO_2:H_2O ratios is thought to reflect variable CO_2:H_2O ratios in primitive liquids. However, fractional crystallization under vapor-saturated conditions would also generate residual liquids with progressively increasing H_2O:CO_2 ratios, so a vapor-saturated liquid line of descent at a single total pressure will also generate a negatively sloped array in a figure such as Fig. 1 (Holloway, 1976; Anderson *et al.*, 1989).

These calculations illustrate the importance of considering simultaneously all of the major volatile species when interpreting trends in dissolved volatile species concentrations in magmas. In particular, as shown in Fig. 1, the concentration of volatile components such as carbon dioxide and water can be highly variable in a series of magmas erupted at a constant pressure, but if the concentration of only one of these volatile components in the glasses were measured, it would be difficult to understand its variability or to confidently attribute it solely to the effects of the presence of other volatile components in the vapor. In the case of the Bishop Tuff, for example, estimated amounts of water in the magma were lower than the amounts that would dissolve if the melt were saturated with pure water vapor at the pressures thought to apply to the magma chamber. This was initially interpreted as signifying that the magma was not vapor saturated (Hildreth, 1977). However, subsequent work has shown that carbon dioxide is present in quenched samples of the magma in sufficient quantities that the magma could have been saturated with a CO_2–H_2O-rich vapor at depth before eruption (Anderson *et al.*, 1989).

Another example of the importance of considering the full suite of volatiles comes from the recent work of Nilsson & Peach (1993), in which they reported Fe^{3+}/Fe^{2+}, SO_4^{2-}/S^{2-} and S contents in a series of vesicular basaltic glasses from the Lau Basin erupted over a narrow depth interval. They observed that S concentration correlates negatively with Fe^{3+}/Fe^{2+}, and inferred that this reflects the decreasing solubility of sulfur with increasing oxygen fugacity; i.e. more oxidized magmas can dissolve less sulfur at a given total pressure than more reduced magmas. There is, however, an alternative interpretation of their observations based on the general form of the isobars shown in Fig. 1. Back-arc basin magmas are often rich in water and contain carbon dioxide in addition to sulfur, and thus the amount of degassing of each of these volatile components at a given

eruption depth depends on the concentrations and solubilities of the other two. As described above, water and carbon dioxide contents of the degassed glasses erupted at a single depth are expected to be inversely correlated if there is a range in H_2O:CO_2 ratios, and this is indeed observed in back-arc basin glasses (Newman, 1989, 1990; Stolper & Newman, 1994). Water and sulfur contents are also expected to be negatively correlated in vapor-saturated glasses as isobars for water and sulfur, though probably differently shaped, must also be negatively sloped under most conditions. In general, regardless of their oxidation state, more water-rich magmas will degas more sulfur and CO_2 at a given depth than water-poor magmas. Consequently, water-rich magmas will have both lower sulfur and lower carbon dioxide contents after degassing, and extensive degassing of carbon dioxide could even lead to more oxidized glasses (Mathez, 1984). However, water contents of back-arc basin magmas are generally higher in more oxidized magmas (Volpe *et al.*, 1987; Hawkins *et al.*, 1990), probably reflecting the slab derivation of water in their source regions. Thus, even if oxidation state had no influence on the solubility of carbon dioxide and sulfur, a negative correlation between Fe^{3+}/Fe^{2+} and both carbon dioxide content and sulfur content would be observed. Although there is a relationship between sulfur solubility and oxidation state (Katsura & Nagashima, 1974; Carroll & Rutherford, 1985; Luhr, 1990; Wallace & Carmichael, 1992) and thus the explanation offered by Nillson and Peach (1993) is plausible and is possibly the dominant control on observed S contents of Lau basin glasses, our point is that it can be misleading to try to evaluate the nature and extent of degassing by examining the variation in concentration of only one volatile component.

VAPOR SATURATION OF SUBMARINE BASALTS

Compositions of vapor in equilibrium with submarine basaltic liquids

As described in the previous section, given measurements of the H_2O and CO_2 contents of natural basaltic glasses, we can determine the pressure at which a liquid of this composition would be vapor saturated and the composition of the equilibrium vapor. This can be done graphically using Fig. 1, or by substituting equations (3) and (4) into equation (2) and then iteratively solving for pressure and using the Lewis–Randall rule to determine vapor composition. In this section, we summarize equilibrium vapor compositions for basaltic glasses and glass inclusions calculated in this way. To avoid discrepancies between different analytical techniques, which are known to be severe for CO_2 measurements (Byers *et al.*, 1986; Des Marais, 1986; Fine & Stolper, 1986; Craig, 1987; Exley *et al.*, 1987), we have restricted our treatment to glasses in which H_2O and CO_2 contents were measured with the same IR spectroscopic technique used to determine the H_2O and CO_2 solubilities (i.e. Fine & Stolper, 1986; Dixon *et al.*, 1988, 1991; Anderson & Brown, 1993; Stolper & Newman, 1994; and unpublished data, 1995).

Figure 2a shows the distribution of the equilibrium vapor compositions for mid-ocean ridge basalt (MORB) liquids based on the H_2O and CO_2 contents of natural MORB glasses. Based on 102 analyses of MORB glasses having water contents ranging from 0·09 to 0·52 wt %, equilibrium vapor compositions range from 0·93 to 1·00 mol fraction CO_2 ($X^v_{CO_2}$); however, most of the glasses (97 out of 102) would be in equilibrium with a vapor having $X^v_{CO_2} > 0{\cdot}95$. Though actual measurements of gas compositions in vesicles in submarine MORB glasses are limited, most measured vapor compositions have $X^v_{CO_2} > 0{\cdot}90$ (Moore *et al.*, 1977; Jambon & Zimmermann, 1987) and are consistent with our calculated compositions. Analyses of gas in vesicles by Pineau & Javoy (1983), however, are more H_2O rich, with mole fractions of CO_2 ranging from 0·03 to 0·85. A possible explanation for the H_2O-rich nature of these vapor compositions is that they represent nonequilibrium compositions, which could develop in rapidly grown bubbles as the result of the higher diffusivity of water compared with CO_2 (e.g. Zhang & Stolper, 1991).

Figure 2b shows the distribution of vapor compositions calculated to be in equilibrium with tholeiitic basaltic liquids from Kilauea volcano, Hawaii, based on the H_2O and CO_2 contents in submarine East Rift Zone glasses (Dixon *et al.*, 1991) and glass inclusions in olivine from Kilauea Iki (Anderson & Brown, 1993). Some samples in both sample suites have CO_2 contents below detection limits; these samples are excluded from the figure because the uncertainty in $X^v_{CO_2}$ based on the uncertainty in the dissolved CO_2 contents is large ($>0{\cdot}5$ absolute). Based on 53 analyses of these glasses having water contents ranging from 0·11 to 0·96 wt %, calculated $X^v_{CO_2}$ values range from 0·60 to 0·99. The mean calculated $X^v_{CO_2}$ in the Kilauean samples (0·91 for the melt inclusions and 0·86 for the East Rift Zone lavas) is less than that for MORB, reflecting the higher water contents typical of ocean island basalts.

Figure 2c shows the equivalent distribution for Mariana back-arc basin (Stolper & Newman, 1994;

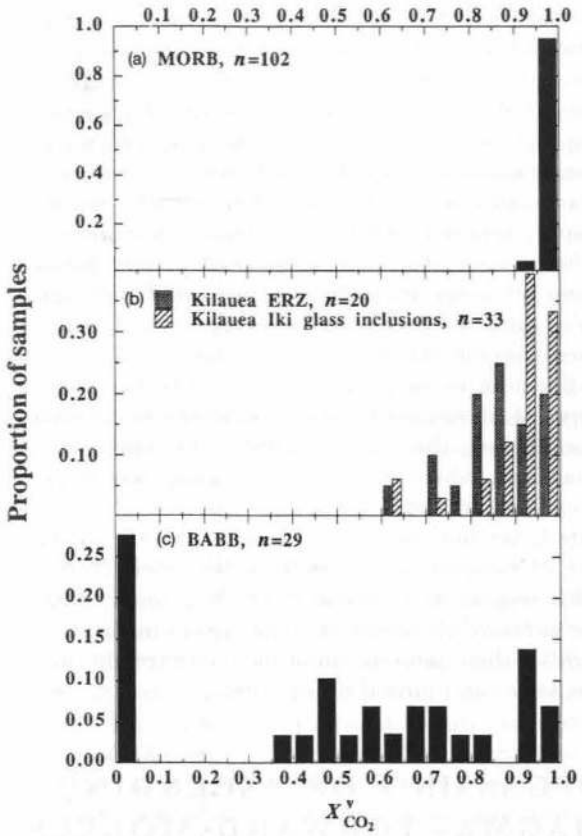

Fig. 2. Calculated vapor compositions for vapor-saturated basaltic melts from different tectonic environments. Vapor compositions were calculated as described in the text by iteratively solving equation (2) for pressure and then using the Lewis–Randall rule (ideal mixing in the vapor phase) to determine vapor composition. (a) MORB (Fine & Stolper, 1986; Dixon *et al.*, 1988, and unpublished data, 1995). Several analyses of partially devitrified glasses from the Juan de Fuca Ridge having CO_2 contents lower than nondevitrified glass from the same sample (Dixon *et al.*, 1988) were omitted. (b) Submarine glasses from the East Rift Zone of Kilauea (Dixon *et al.*, 1991) and glass inclusions in olivine from the 1958 eruption of Kilauea Iki (Anderson & Brown, 1993). Though some samples from Kilauea (4 out of 24 from KERZ and 17 out of 50 from Kilauea Iki) have CO_2 concentrations below detection limits, the uncertainty in $X^v_{CO_2}$ based on the uncertainty in CO_2 concentrations is >0·5 (absolute) in all cases and vapor compositions based on these analyses are not shown. (c) Back-arc basin basaltic glasses from the Mariana back-arc basin (Newman *et al.*, 1993; Stolper & Newman, 1994). Based on the uncertainty in the CO_2 analyses in the three samples having CO_2 concentrations below detection limits, the uncertainty in the $X^v_{CO_2}$ is <0·1 absolute.

S. Newman, unpublished data, 1995). As expected, the calculated vapor phase compositions are more variable and water rich ($X^v_{CO_2}$ ranges from zero, with uncertainties of up to 0·1 absolute, to 0·94, with a mean of 0·46) for these samples, which have water contents that are more variable and typically higher (0·49–2·14 wt %) than those of MORB glasses (Delaney *et al.*, 1978; Muenow *et al.*, 1990).

Pressures of vapor saturation of submarine liquids—comparison with eruption pressures

Pressures of vapor saturation for liquids with the H_2O and CO_2 contents of natural basaltic glasses have also been calculated as described above; these are compared in Fig. 3 with eruption pressures (assuming that the collection depth is equivalent to the eruption depth). Samples plotting on the 1:1 line are consistent with having been saturated with respect to vapor under the conditions of eruption;

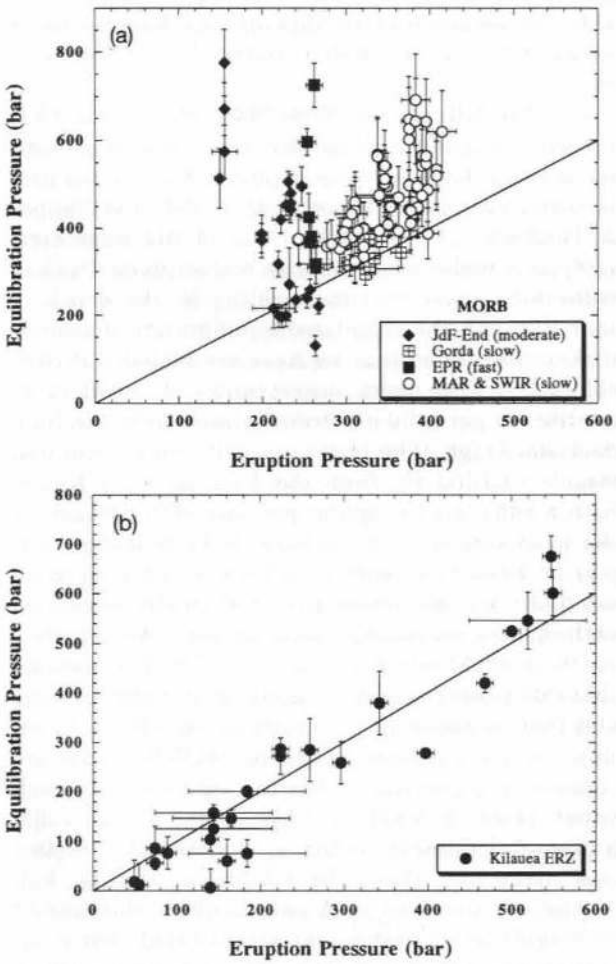

Fig. 3. Calculated pressure of equilibration versus eruption pressure for (a) MORB and (b) Kilauea submarine east rift glasses. Pressures of equilibration are calculated as described in the text by iteratively solving equation (2) for pressure using measured H_2O and CO_2 contents. Errors in eruption pressure (*x*-axis) are based on uncertainties in depths of sample collection. Errors in equilibration pressure (*y*-axis) are based on uncertainties in measured CO_2 concentrations. Sources of data: Juan de Fuca and Endeavour Ridges (JdF-End) from Dixon *et al.* (1988); Gorda Ridge, East Pacific Rise (EPR), Mid-Atlantic Ridge and Southwest Indian Rift from J. Dixon (unpublished data, 1995); Kilauea East Rift Zone (KERZ) from Dixon *et al.* (1991); Kilauea Iki glass inclusions from Anderson & Brown (1993).

those plotting above and below the 1:1 line appear to be supersaturated and undersaturated, respectively, with respect to vapor. For MORBs (Fig. 3a), in which the equilibrium vapor is nearly pure CO_2, the same information can be read from the CO_2 vs total pressure figures presented by Stolper & Holloway (1988) and Dixon *et al.* (1988), where the curve for saturation with respect to CO_2 vapor provides an excellent approximation to the vapor-saturation boundary. However, for samples from back-arc basins and ocean islands, which are often calculated to be saturated with water-rich vapor (Figs. 2b and c), the representation shown in Fig. 3 is more reliable for evaluating whether or not basaltic melts would be vapor saturated under the conditions of eruption.

For MORB glasses, those with the lowest CO_2 contents at a given depth are vapor saturated with respect to a CO_2-rich vapor phase (Fig. 3a), as previously observed by Dixon *et al.* (1988) and Stolper & Holloway (1988). Only 1 out of 102 ridge crest samples is undersaturated with respect to its depth of collection, given the uncertainties in the depth of sampling and the calculated equilibration pressures; it should be noted that we have not included dredge collections with depth uncertainties of >600 m or analyses of partially devitrified glasses from the Juan de Fuca Ridge. The one apparently undersaturated sample (TT152-13, from the Juan de Fuca Ridge, with a calculated eruption pressure of ~130 bar) is the most vesicular of the Juan de Fuca Ridge samples (2·3 vol % vesicles vs <1·8 vol % for all other samples); as high vesicularity is typically associated with shallow submarine eruptions (e.g. Moore, 1965, 1970, 1979; Moore & Schilling, 1973), it is possible that this sample actually erupted at a shallower level and that its apparent undersaturation reflects downslope movement after eruption. MORB glasses are commonly supersaturated with respect to CO_2-rich vapor (Fine & Stolper, 1986; Dixon *et al.*, 1988; Stolper & Holloway, 1988), as evidenced by the fact that many plot above the 1:1 line in Fig. 3a. Following our previous work, we attribute this feature to magma ascent rates that are so rapid that magmas erupt on the sea-floor without having been fully degassed by bubble nucleation and growth during ascent. This feature is present in samples from spreading centers ranging from slow (e.g. the Mid-Atlantic Ridge) to fast (e.g. East Pacific Rise, 9–13°N).

In contrast to the MORB glasses, liquids with the volatile contents of most glasses from the submarine portion of Kilauea's East Rift Zone plot near the 1:1 line in Fig. 3b, and thus are consistent with having been in equilibrium with a vapor phase containing 60–100 mol % CO_2 at the pressure of eruption. Dixon *et al.* (1991) concluded that these glasses were in equilibrium with a CO_2-rich vapor phase, but the use of a new solubility function for CO_2 and the explicit consideration of the presence of water in these samples (some of which are relatively rich in water and would be saturated with a water-rich vapor) represent improvements over previous work. The absence of a large number of glasses quenched from melts significantly supersaturated with respect to a vapor phase distinguishes these Hawaiian samples from the MORB suite, and this probably reflects differences in magma transport rates in these two types of rift environments or very shallow, subsurface (i.e. below the water–volcano interface) storage chambers where extensive degassing occurs before eruption. In the latter case, eruption can still be rapid, yet not show gross supersaturation. A few of the 24 samples appear to have been undersaturated with respect to a mixed H_2O–CO_2 vapor phase at the pressure of collection; as suggested by Dixon *et al.* (1991), these samples could have erupted up to 1 km shallower and flowed downslope.

DEGASSING OF ASCENDING MAGMA—FORWARD MODELS

The solubility relations determined in this study can be used to model degassing paths of H_2O–CO_2-bearing basaltic magmas for a variety of conditions relevant to submarine and subaerial eruptions. The modeling presented here is based on an approach developed by Dr G. Miller (University of Chicago) and Dr P. Dobson (Unocal) and described in the Appendix. Our modeling produces results similar to previous degassing calculations by Khitarov & Kadik (1973), Shilobreyeva *et al.* (1983), Gerlach (1986), Newman (1989, 1990) and Bottinga & Javoy (1990*b*) for basaltic systems, and by Holloway (1976) and Newman *et al.* (1988) for rhyolitic systems, although our calculations are based specifically on our thermodynamic models for water and carbon dioxide solubility in MORB liquids at 1200°C .

Degassing during decompression is modeled in successive isobaric steps. At each pressure, H_2O and CO_2 dissolved in the supersaturated melt are 'transferred' incrementally into the vapor phase until saturation is reached. The relative proportion of water and CO_2 partitioned into the vapor phase during each incremental transfer is determined by solving simultaneously equations describing mass balance, H_2O speciation, and equilibrium partitioning of CO_2 and H_2O between vapor and melt $[(X^v_{CO_2}/X^v_{H_2O})/(X^m_{CO_3^{2-}}/X^m_{H_2O,mol})]$. The pressure is then

incremented downward, leading again to a supersaturated melt, and the calculation is repeated. Both open and closed system degassing calculations were performed. In open system degassing, the vapor phase is instantaneously removed from the magma after each increment of volatile loss. In closed system degassing, the vapor phase remains in contact and equilibrium with the melt, increasing in amount and changing in composition with each increment of volatile loss from the liquid. In both cases, the composition of the degassed magma and the proportion and the composition of the vapor phase (integrated vapor composition for closed system and instantaneous vapor composition for open system degassing) were calculated over the range of pressures relevant to seafloor degassing.

Open system degassing

Because removal of the vapor from the system after each degassing step causes a loss of 'memory' of the initial conditions as degassing proceeds, open system degassing paths during decompression are independent of the path by which a batch of melt arrived at its concentrations of H_2O and CO_2. During open system degassing, CO_2 is rapidly removed from the melt with negligible loss of water, until a pressure is reached at which the melt is in equilibrium with nearly pure water vapor. With further reduction in pressure, the concentration of water in the melt follows almost exactly the water solubility curve. Open system degassing paths (Fig. 4) are virtually identical for melts having the same initial H_2O contents but highly variable initial CO_2 contents, consistent with the results of Holloway (1976), Shilobreyeva *et al.* (1983) and Newman *et al.* (1988). For example, during open system degassing of melts with initial water contents of 1 wt % to a pressure of 100 bar, the melts lose only 2% of their initial water, regardless of their initial CO_2/H_2O ratio. That CO_2 is so strongly partitioned into the vapor is important because even if only a small amount of vapor exsolves from an ascending melt, it will be extremely difficult to deduce the initial CO_2 content of the magma by measuring the CO_2 content of the quenched glass.

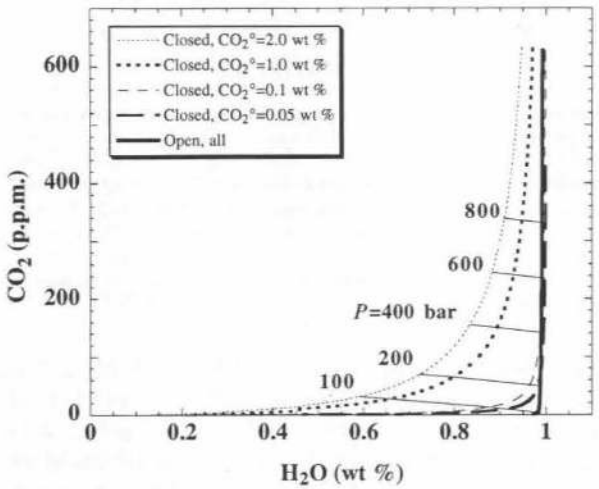

Fig. 4. Difference in model degassing paths for open and closed systems and the effect of CO_2 content on closed system degassing for basaltic liquids having an initial H_2O content of 1·0 wt % and initial CO_2 contents of 0·05, 0·1, 1·0 and 2·0 wt % (initial CO_2/H_2O mass ratios of 0·05, 0·1, 1·0 and 2·0). All calculations begin degassing at 1200 bar. Curves of constant pressure (isobars) illustrate how the H_2O and CO_2 concentrations at vapor saturation vary with initial volatile concentrations during closed system degassing.

Closed system degassing

During closed system degassing, the vapor remains in contact with the melt and thus 'remembers' the initial volatile content of the melt. As emphasized by Holloway (1976) and Newman *et al.* (1988), the water content in a vapor-saturated melt undergoing closed system degassing will be strongly dependent on the initial CO_2 content, especially at high total volatile concentrations and high CO_2:H_2O ratios. The effects of varying the initial CO_2 at constant initial H_2O concentrations in closed system degassing are illustrated in Fig. 4. Calculations were done for melts having an initial H_2O content of 1·0 wt % and initial CO_2 contents of 500 p.p.m., 1000 p.p.m., 1 wt % and 2 wt %. During closed system degassing to a pressure of 100 bar, a basaltic liquid initially having 1·0 wt % H_2O and 500 p.p.m. CO_2 will lose only 8% of its initial water; whereas a melt initially having 1 wt % H_2O and 2 wt % CO_2 will lose almost 40% of its initial water. It should be noted that for initial H_2O and CO_2 contents typical of tholeiites erupted on ocean islands and along mid-ocean ridges, the calculated differences between open and closed system degassing paths are small (Fig. 4). Differences in H- and C-isotopic ratios of the residual melts, however, would be more strongly dependent on the style of degassing (e.g. Newman *et al.*, 1988; Gerlach & Taylor, 1990).

Figures 5a–d show the calculated variations of H_2O and CO_2 contents in the melt and in the vapor with pressure during closed system degassing of basaltic liquids for basaltic liquids having initial CO_2 contents of 500 p.p.m. and different initial H_2O contents ranging from 0·1 to 2·0 wt %. The range of water contents covers the typical range found in basaltic magmas from mid-ocean ridges and back-arc basins (Moore & Schilling, 1973; Moore *et al.*, 1977; Delaney *et al.*, 1978; Garcia *et al.*, 1979; Moore, 1979; Muenow *et al.*, 1980, 1990; Byers *et al.*, 1983, 1984,

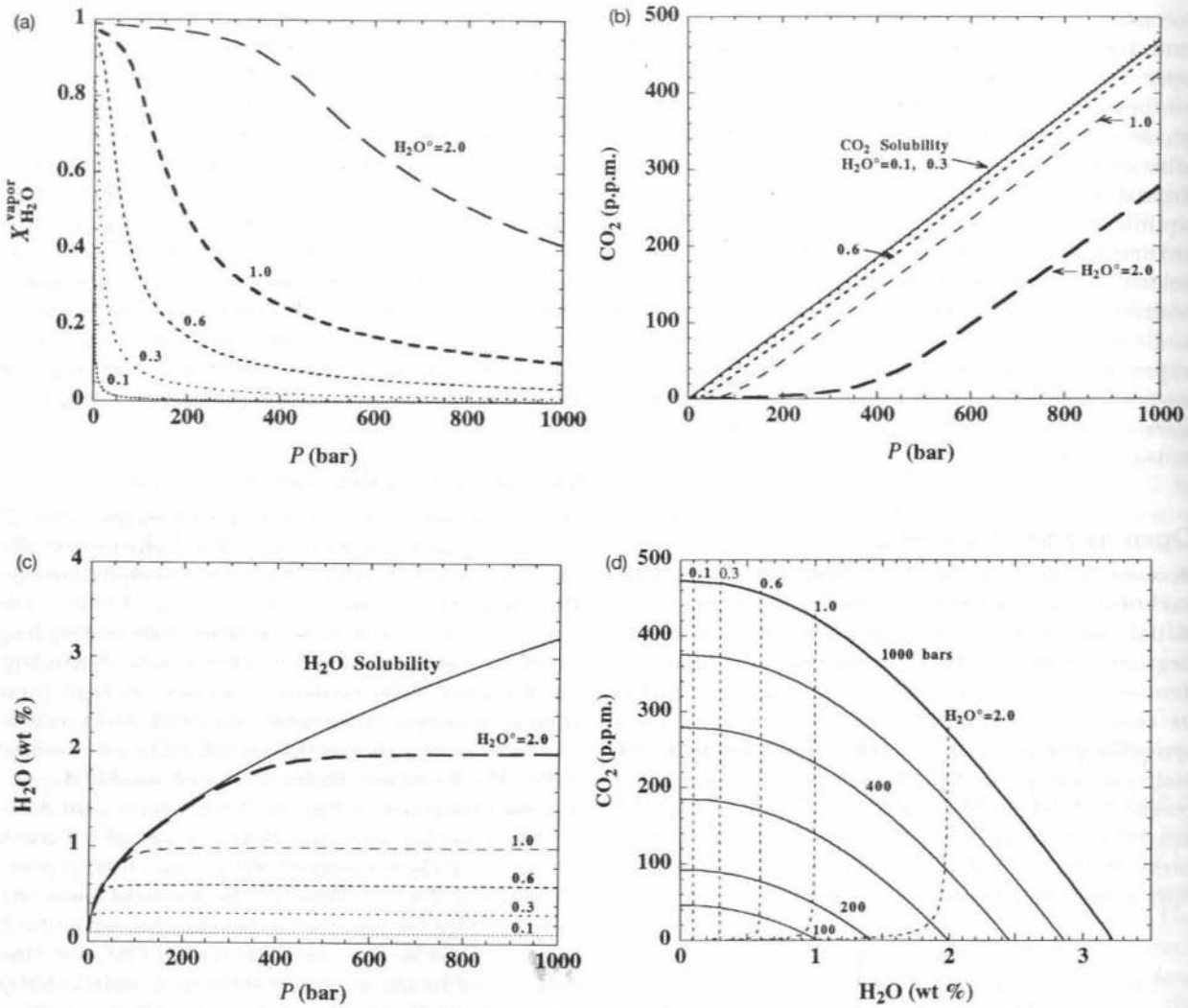

Fig. 5. (a) Results of closed system degassing calculations showing the variation in composition of mixed H_2O–CO_2 vapor phase in equilibrium with basaltic melts having an initial CO_2 content of 500 p.p.m. and a range of initial H_2O contents. Numbers next to curves represent initial water content of magma. (b) CO_2 vs P_{Total} in vapor-saturated basaltic melts initially containing 500 p.p.m. CO_2 and a range of H_2O contents (0·1–2·0 wt %) degassed under closed system conditions at 1200°C. The trends for melts containing 0·1 and 0·3 wt % H_2O cannot be distinguished from the trend for pure CO_2 solubility ($P_{Total} = P_{CO_2}$; continuous line) at this scale. (c) H_2O vs P in vapor-saturated basaltic melts for closed system degassing of melts initially containing 500 p.p.m. CO_2 and a range of H_2O contents (0·1–2·0 wt %). Continuous line is solubility of water in equilibrium with pure water vapor (i.e. for $P_{Total} = P_{H_2O}$). Dashed lines are degassing paths for melts with different initial water concentrations. (d) Closed system degassing paths (dashed lines) superposed on isobars from Fig. 1 for basaltic liquids.

1986; Fine & Stolper, 1986; Michael & Chase, 1987; Dixon *et al.*, 1988; Michael, 1988; Jendrzejewski *et al.*, 1992; Danyushevsky *et al.*, 1993; Stolper & Newman, 1994). Liquids with these compositions will be vapor saturated in a magma chamber located at a depth of ~2–4 km beneath the ocean floor where total pressure ranges from ~700 to 1200 bar.

At 1000 bar, the vapor in these examples is rich in CO_2 compared with H_2O (though the vapor in the case with 2 wt % initial water is almost 50 mol % H_2O) and becomes progressively enriched in water as pressure decreases (Fig. 5a). The CO_2 content of the melt decreases approximately linearly with a slope similar to that of the CO_2 solubility curve (Fig. 5b) from the point at which vapor saturation is reached until nearly all of the CO_2 has been partitioned into the vapor. Figure 5b also shows that at a given pressure, the content of CO_2 dissolved in the vapor-saturated melt decreases with initial water content.

In contrast to the behavior of carbon dioxide, the behavior of water during closed system degassing is similar to the open system case in that loss of water owing to degassing is minor until the pressure has dropped to a value near that at which a melt con-

taining no carbon dioxide, but with same initial water content, would be saturated with pure water vapor (Fig. 5c). The calculations shown in Figs. 5b and c can be coupled and added to Fig. 1 to show the covariation of CO_2 and H_2O in melts during closed system degassing of these submarine magma compositions (Fig. 5d). The dashed lines illustrate the dramatic decrease in CO_2 content with negligible change in water content as magmas degas during depressurization. These calculations (all having initial CO_2 contents of 500 p.p.m.) show that H_2O concentrations in typical MORB (~0·1–0·3 wt% H_2O) will not be significantly modified (<10% of total water exsolved as vapor) by degassing during eruption on the sea-floor unless erupted in water depths shallower than ~100 m. Tholeiites from oceanic islands and MORB enriched in incompatible elements (E-MORB) containing higher water contents (~0·3–1·0%) can begin exsolving significant amounts of H_2O at eruption depths of 100–1000 m. Thus, water contents in quenched MORB and ocean-island tholeiitic glasses can be used reliably to obtain original (i.e. largely unaffected by degassing) water contents as long as they were erupted in water deeper than 1000 m. The pressure at which 50% loss of water has occurred is 2, 8, 22 and 98 bar for initial water contents of 0·3, 0·6, 1·0 and 2·0 wt%, respectively. Water concentrations in water-rich arc or back-arc related magmas, however, may be as high as 6 wt% (Gaetani *et al.*, 1993; Sisson & Layne, 1993; S. Newman, personal communication, 1994). Exsolution of an H_2O-rich vapor from these water-rich magmas and production of highly vesicular lavas will occur even at water depths >2000 m (P > 200 bar). Thus, the presence of high vesicularity does not necessarily indicate eruption at shallow depth (see Dudas, 1983). Degassing of an H_2O-rich vapor in arc environments may begin at depth in the crust, probably within the magma chamber (e.g. Stix *et al.*, 1993).

SUMMARY

Our experimental results on water and carbon dioxide solubilities in basaltic melts provide a basis for interpreting the water and carbon contents of submarine magmas and for assessing factors controlling degassing on ascent and emplacement. They can be used to determine the pressure at which a basaltic liquid with known concentrations of water and carbon dioxide would be vapor saturated at 1200°C and the composition of the vapor phase with which it would be saturated under these conditions. Suites of quenched basaltic melts erupted over a narrow depth interval but having a range of initial CO_2/H_2O ratios will define negatively sloped arrays on an H_2O vs CO_2 plot. It is important that all of the major volatile species should be considered simultaneously when interpreting trends in dissolved volatile species concentrations in magmas.

Vapor compositions in equilibrium with submarine tholeiitic glasses have been calculated for glasses in which H_2O and CO_2 were analyzed using IR spectroscopy. The range in equilibrium vapor compositions [$X^v_{CO_2}$ = 0·93–1·00 for MORB, 0·60–0·99 for Kilauea (OIB) and 0–0·94 for BABB] reflects the range in water contents in the melts characteristic of each environment. MORB glasses from spreading centers ranging from slow (e.g. the Mid-Atlantic Ridge) to fast (e.g. East Pacific Rise, 9–13°N) are commonly supersaturated with respect to CO_2-rich vapor, resulting from magma ascent rates so rapid that magmas erupt on the sea-floor without having been fully degassed by bubble nucleation and growth during ascent (Dixon *et al.*, 1988; Stolper & Holloway, 1988). Volatile contents in submarine glasses from Kilauea, however, are consistent with having been in equilibrium with a vapor phase containing 60–100 mol% CO_2 at the pressure of eruption, suggesting that the total time of magma transport from magma chamber to sea-floor is longer for eruptions ocurring along the submarine extensions of hotspot volcanic rift zones than along mid-ocean ridges.

Degassing during decompression of tholeiitic basaltic melts is characterized by strong partitioning of CO_2 into the vapor phase. During open system degassing, CO_2 is rapidly removed from the melt with negligible loss of water, until a pressure is reached at which the melt is in equilibrium with nearly pure water vapor. From this pressure downward, the water content of the melt follows the water solubility curve. During closed system degassing, water and CO_2 contents in vapor-saturated basaltic magmas will depend strongly on the vapor composition as determined by the initial volatile concentrations. Deviation from open system behavior, toward lower dissolved H_2O and CO_2 saturation concentrations at a given pressure, will be greatest in melts having high total volatile concentrations and high CO_2:H_2O ratios. Closed system degassing of basaltic melts having the low initial H_2O and CO_2 contents typical of MORB and OIB, however, are similar to the open system case.

ACKNOWLEDGEMENTS

This work was supported by NSF Grants EAR-8811406, EAR-8617128 and OCE88-20131. We thank Patrick Dobson, John Holloway, Greg Miller and Sally Newman for assistance and advice. Thoughtful reviews by P. Ihinger and an anonymous

reviewer are gratefully acknowledged. This paper is Caltech Division of Geological and Planetary Sciences Contribution 5484.

REFERENCES

Anderson, A. T., 1974. Chlorine, sulfur, and water in magmas and oceans. *Geological Society of America Bulletin* **85,** 1485–1492.

Anderson, A. T. & Brown, G. G., 1993. CO_2 contents and formation pressures of some Kilauean melt inclusions. *American Mineralogist* **78,** 794–803.

Anderson, A. T., Newman, S., Williams, S. N., Druitt, T. H., Skirius, C. & Stolper, E., 1989. H_2O, CO_2, Cl, and gas in Plinian and ash-flow Bishop rhyolite. *Geology* **17,** 221–225.

Bottinga, Y. & Javoy, M., 1990*a*. Mid-ocean ridge basalt degassing: bubble nucleation. *Journal of Geophysical Research* **95,** 5125–5131.

Bottinga, Y. & Javoy, M., 1990*b*. MORB degassing: bubble growth and ascent. *Chemical Geology* **81,** 255–270.

Brantley, S., Ágústsdóttir, A. M. & Rowe, G.L., 1993. Crater Lakes reveal volcanic heat and volatile fluxes. *GSA Today* **3**(7), 173–178.

Byers, C. D., Muenow, D. W. & Garcia, M. O., 1983. Volatiles in basalts and andesites from the Galapagos spreading center, 85° to 86°W. *Geochimica et Cosmochimica Acta* **47,** 1551–1558.

Byers, C. D., Christie, D. M., Muenow, D. W. & Sinton, J. M., 1984. Volatile contents and ferric–ferrous ratios of basalt, ferrobasalt, andesite and rhyodacite glasses from the Galapagos 95·5°W propagating rift. *Geochimica et Cosmochimica Acta* **48,** 2239–2245.

Byers, C. D., Garcia, M. O. & Muenow, D. W., 1986. Volatiles in basaltic glasses from the East Pacific Rise at 21°N: implications for MORB sources and submarine lava flow morphology. *Earth and Planetary Science Letters* **79,** 9–20.

Carroll, M. R. & Rutherford, M. J., 1985. Sulfide and sulfate saturation in hydrous silicate melts. *Journal of Geophysical Research* **90,** C601–C612.

Craig, H., 1987. Comment on "Carbon isotope systematics of a mantle hotspot: a comparison of Loihi Seamount and MORB glasses" by R. A. Exley, D. P. Mattey, D. A. Clague and C. T. Pillinger. *Earth and Planetary Science Letters* **82,** 384–386.

Danyushevsky, L. V., Falloon, T. J., Sobolev, A. V., Crawford, A. J., Carroll, M. & Price, R. C., 1993. The H_2O content of basalt glasses from Southwest Pacific back-arc basins. *Earth and Planetary Science Letters* **117,** 347–362.

Delaney, J. R., Muenow, D. W. & Graham, D. G., 1978. Abundance and distribution of water, carbon and sulfur in the glassy rims of submarine pillow basalts. *Geochimica et Cosmochimica Acta* **42,** 581–594.

Des Marais, D. J., 1985. Carbon exchange between the mantle and the crust, and its effect upon the atmosphere: today compared to Archean time. *Geophysical Monograph, American Geophysical Union* **32,** 602–611.

Des Marais, D. J., 1986. Carbon abundance measurements in oceanic basalts: the need for a consensus. *Earth and Planetary Science Letters* **79,** 21–26.

Devine, J. D., Sigurdsson, H. & Davis, A. N., 1984. Estimates of sulfur and chlorine yield to the atmosphere from volcanic eruptions and potential climatic effects. *Journal of Geophysical Research* **89,** 6309–6325.

Dixon, J. E., Stolper, E. & Delaney, J. R., 1988. Infrared spectroscopic measurements of CO_2 and H_2O glasses in the Juan de Fuca Ridge basaltic glasses. *Earth and Planetary Science Letters* **90,** 87–104.

Dixon, J. E., Clague, D. A. & Stolper, E. M., 1991. Degassing history of water, sulfur, and carbon in submarine lavas from Kilauea volcano, Hawaii. *Journal of Geology* **99,** 371–394.

Dixon, J. E., Stolper, E. M. & Holloway, J. R., 1995. An experimental study of water and carbon dioxide solubilities in mid-ocean ridge basaltic liquids. Part I: Calibration and solubility models. *Journal of Petrology* **36,** 1607–1631.

Dudas, F. Ö., 1983. The effect of volatile content on the vesiculation of submarine basalts. *Economic Geology, Monograph* **5,** 134–141.

Exley, R. A., Mattey, D. P. & Pillinger, C. T., 1987. Low temperature carbon components in basaltic glasses—reply to comment by H. Craig. *Earth and Planetary Science Letters* **82,** 387–390.

Fine, G. & Stolper, E., 1986. Carbon dioxide in basaltic glasses: concentrations and speciation. *Earth and Planetary Science Letters* **76,** 263–278.

Gaetani, G. A., Grove, T. L. & Bryan, W. B., 1993. The influence of water on the petrogenesis of subduction-related igneous rocks. *Nature* **365,** 332–334.

Garcia, M. O., Liu, N. W. K. & Muenow, D. W., 1979. Volatiles in submarine volcanic rocks from the Mariana Island arc and trough. *Geochimica et Cosmochimica Acta* **43,** 305–312.

Gerlach, T. M., 1986. Exsolution of H_2O, CO_2, and S during eruptive episodes at Kilauea Volcano, Hawaii. *Journal of Geophysical Research* **91,** 12177–12185.

Gerlach, T. M., 1989. Degassing of carbon dioxide from basaltic magma at spreading centers: II. Mid-oceanic ridge basalts. *Journal of Volcanology and Geothermal Research* **39,** 221–232.

Gerlach, T. M. & Casadevall, T. J., 1986. Fumarole emissions at Mount St. Helens volcano, June 1980 to October 1981: degassing of a magma–hydrothermal system. *Journal of Volcanology and Geothermal Research* **28,** 141–160.

Gerlach, T. M. & Graeber, E. J., 1985. Volatile budget of Kilauea volcano. *Nature* **313,** 273–277.

Gerlach, T. M. & Taylor, B., 1990. Carbon isotope constraints on degassing of carbon dioxide from Kilauea Volcano. *Geochimica et Cosmochimica Acta* **54,** 2051–2058.

Hawkins, J. W., Lonsdale, P. F., Macdougall, J. D. & Volpe, A. M., 1990. Petrology of the axial ridge of the Mariana Trough backarc spreading center. *Earth and Planetary Science Letters* **100,** 226–250.

Heilbornn, J., 1981. *Science and Engineering Programs.* Osborne–McGraw–Hill, Berkeley, CA, 223 pp.

Hildreth, E. W., 1977. The magma chamber of the Bishop Tuff: gradients in temperature, pressure and composition. Ph.D. Thesis, University of California, Berkeley, 328 pp.

Holloway, J. R., 1976. Fluids in the evolution of granitic magmas: consequences of finite CO_2 solubility. *Geological Society of America Bulletin* **87,** 1513–1518.

Holloway, J. R., 1977. Fugacity and activity of molecular species in supercritical fluids. In: Fraser, D. (ed.) *Thermodynamics in Geology.* Boston, MA: D. Reidel, pp. 161–181.

Jagger, T. A., 1940. Magmatic gases. *American Journal of Science* **238,** 313–353.

Jambon, A., 1994. Earth degassing and large-scale geochemical cycling of volatile elements. In: Carroll, M. R. & Holloway, J. R. (eds) *Volatiles in Magmas. Reviews in Mineralogy, Mineralogical Society of America* **30,** 479–517.

Jambon, A. & Zimmermann, J. L., 1987. Major volatiles from a North Atlantic MORB glass and calibration to He: a size fraction analysis. *Chemical Geology* **62,** 177–189.

Jaupart, C. & Vergniolle, S., 1988. Laboratory models of Hawaiian and Strombolian eruptions. *Nature* **331,** 58–60.

Jaupart, C. & Vergniolle, S., 1989. The generation and collapse of a foam layer at the roof of a basaltic magma chamber. *Journal of Fluid Mechanics* **203,** 347–380.

Javoy, M., Pineau, F. & Allègre, C. J., 1982. Carbon geodynamical cycle. *Nature* **300,** 171–173.

Jendrzejewski, N., Pineau, F. & Javoy, M., 1992. Water and carbon contents and isotopic compositions in Indian Ocean MORB. *Eos Transactions of the American Geophysical Union* **73,** *Spring Meeting Supplement*, 352.

Katsura, T. & Nagashima, S., 1974. Solubility of sulfur in some magmas at 1 atmosphere. *Geochimica et Cosmochimica Acta* **38,** 517–531.

Khitarov, N. I. & Kadik, A. A., 1973. Water and carbon dioxide in magmatic melts and peculiarities of the melting process. *Contributions to Mineralogy and Petrology* **41,** 205–215.

Kodosky, L. G., Motyka, R. J. & Symonds, R. B., 1991. Fumarolic emissions from Mount St. Augustine, Alaska: 1979–1984 degassing trends, volatile sources and their possible role in eruptive style. *Bulletin of Volcanology* **53,** 381–394.

Le Guern, F., Carbonnelle, J. & Tazieff, H., 1979. Erta'ale lava lake: heat and gas transfer to the atmosphere. *Journal of Volcanology and Geothermal Research* **6,** 27–48.

Luhr, J. F., 1990. Experimental phase relations of water- and sulfur-saturated arc magmas and the 1982 eruptions of El Chichón Volcano. *Journal of Petrology* **31,** 1071–1114.

Mangan, M. T., Cashman, K. V. & Newman, S., 1993. Vesiculation of basaltic magma during eruption. *Geology* **21,** 157–160.

Marty, B. & Jambon, A., 1987. $C/^3He$ in volatile fluxes from the solid Earth: implications for carbon geodynamics. *Earth and Planetary Science Letters* **83,** 16–26.

Mathez, E. A., 1984. Influence of degassing on oxidation states of basaltic magmas. *Nature* **310,** 371–375.

Michael, P. J., 1988. The concentration, behavior and storage of H_2O in the suboceanic upper mantle: implications for mantle metasomatism. *Geochimica et Cosmochimica Acta* **52,** 555–566.

Michael, P. J. & Chase, R. L., 1987. The influence of primary magma composition, H_2O and pressure on mid-ocean ridge basalt differentiation. *Contributions to Mineralogy and Petrology* **96,** 245–263.

Michael, P. J. & Schilling, J.-G., 1989. Chlorine in mid-ocean ridge magmas: evidence for assimilation of seawater influenced components. *Geochimica et Cosmochimica Acta* **53,** 3131–3143.

Moore, J. G., 1965. Petrology of deep-sea basalt near Hawaii. *American Journal of Science* **263,** 40–52.

Moore, J. G., 1970. Water content of basalt erupted on the ocean floor. *Contributions to Mineralogy and Petrology* **28,** 272–279.

Moore, J. G., 1979. Vesicularity and CO_2 in mid-ocean ridge basalt. *Nature* **282,** 250–253.

Moore, J. G. & Schilling, J.-G., 1973. Vesicles, water, and sulfur in Reykjanes Ridge basalts. *Contributions to Mineralogy and Petrology* **41,** 105–118.

Moore, J. G., Batchelder, J. N. & Cunningham, C. G., 1977. CO_2-filled vesicles in mid-ocean basalt. *Journal of Volcanology and Geothermal Research* **2,** 309–327.

Muenow, D. W., Liu, N. W. K., Garcia, M. O. & Saunders, A. D., 1980. Volatiles in submarine volcanic rocks from the spreading axis of the East Scotia Sea back-arc basin. *Earth and Planetary Science Letters* **47,** 272–278.

Muenow, D. W., Garcia, M. O., Aggrey, K. W., Bednaez, U. & Schmincke, H. U., 1990. Volatiles in submarine glasses as a discriminant of tectonic origin: application to the Troodos ophiolite. *Nature* **343,** 159–161.

Newman, S., 1989. Water and carbon dioxide contents in basaltic glasses from the Mariana Trough. *Eos Transactions of the American Geophysical Union* **70,** *Fall Meeting Supplement*, 1387.

Newman, S., 1990. Water and carbon dioxide contents of back arc basin basalts. *V. M. Goldschmidt Conference 1990 Programs and Abstracts*, p. 69.

Newman, S., Epstein, S., & Stolper, E., 1988. Water, carbon dioxide, and hydrogen isotopes in glasses from the ca. 1340 A.D. eruption of the Mono Craters, California: constraints on degassing phenomena and initial volatile content. *Journal of Volcanology and Geothermal Research* **35,** 75–96.

Nilsson, K. & Peach, C., 1993. Sulfur speciation as a function of magmatic oxidation state: implications for sulfur concentrations in backarc and island arc magmas. *Geochimica et Cosmochimica Acta* **57,** 3807–3813.

Palais, J.M. & Sigurdsson, H., 1989. Petrologic evidence of volatile emissions from major historic and pre-historic volcanic eruptions. *Geophysical Monograph, American Geophysical Union* **52,** 31–53.

Pineau, F. & Javoy, M., 1983. Carbon isotopes and concentrations in mid-oceanic ridge basalts. *Earth and Planetary Science Letters* **62,** 239–257.

Schilling, J.-G., Bergeron, M. B. & Evans, R., 1980. Halogens in the mantle beneath the North Atlantic. *Philosophical Transactions of the Royal Society of London, Series A* **297,** 147–178.

Schilling, J.-G., Zajac, M., Evans, R., Johnston, R., White, W., Devine, J. D. & Kingsley, R., 1983. Petrologic and geochemical variations along the Mid-Atlantic Ridge from 29°N to 73°N. *American Journal of Science* **283,** 510–586.

Shilobreyeva, S. N., Kadik, A. A. & Lukanin, O. A., 1983. Outgassing of ocean-floor magma as a reflection of volatile conditions in the magma generation region. *Geokhimiya* **9,** 1257–1274.

Silver, L. A., Ihinger, P. D. & Stolper, E. M., 1990. The influence of bulk composition on the speciation of water in silicate glasses. *Contributions to Mineralogy and Petrology* **104,** 142–162.

Sisson, T. W. & Layne, G. D., 1993. H_2O in basalt and basaltic andesite glass inclusions from four subduction-related volcanoes. *Earth and Planetary Science Letters* **117,** 619–635.

Stix, J., Zapata, G. J. A., Calvache, V. M., Cortés, J. G. P., Fischer, T. P., Gomez, M. D., Naraez, M. L., Ordoñez, V. M., Ortega, E. A., Torres, C. R. & Williams, S. N., 1993. A model of degassing, at Galeras Volcano, Colombia, 1988–1993. *Geology* **21,** 963–967.

Stoiber, R. E., Williams, S. N. & Huebert, B., 1987. Annual contribution of sulfur dioxide to the atmosphere by volcanoes. *Journal of Volcanology and Geothermal Research* **33,** 1–8.

Stolper, E. M. & Holloway, J. R., 1988. Experimental determination of the solubility of carbon dioxide in molten basalt at low pressure. *Earth and Planetary Science Letters* **87,** 397–408.

Stolper, E. M. & Newman, S., 1994. The role of water in the petrogenesis of Mariana trough magmas. *Earth and Planetary Science Letters* **121,** 293–325.

Symonds, R. B., Reed, M. H. & Rose, W. I., 1992. Origin, speciation, and fluxes of trace-element gases at Augustine volcano, Alaska: insights into magma degassing and fumarolic processes. *Geochimica et Cosmochimica Acta* **56,** 633–657.

Tait, S., Jaupart, C. & Vergniolle, S., 1989. Pressure, gas content and eruption periodicity of a shallow, crystallizing magma chamber. *Earth and Planetary Science Letters* **92,** 107–123.

Vergniolle, S. & Jaupart, C., 1986. Separated two-phase flow and basaltic eruptions. *Journal of Geophysical Research* **91,** 12842–12860.

Vergniolle, S. & Jaupart, C., 1990. Dynamics of degassing at Kilauea Volcano, Hawaii. *Journal of Geophysical Research* **95,** 2793–2809.

Volpe, A. M., Macdougall, J. D. & Hawkins, J. W., 1987. Mariana Trough basalts (MTB): trace element and Sr–Nd isotopic evidence for mixing between MORB-like and arc-like melts. *Earth and Planetary Science Letters* **82,** 241–254.

Wallace, P. & Carmichael, I. S.., 1992. Sulfur in basaltic magmas. *Geochimica et Cosmochimica Acta* **56,** 1863–1874.

Williams, S. N., Schaefer, S. J., Calvache V., M. L. & Lopez, D., 1992. Global carbon dioxide emission to the atmosphere by volcanoes. *Geochimica et Cosmochimica Acta* **56,** 1765–1770.

Zhang, Y. & Stolper, E. M., 1991. Water diffusion in a basaltic melt. *Nature* **351,** 306–309.

RECEIVED JANUARY 15, 1994
REVISED TYPESCRIPT ACCEPTED JANUARY 10, 1995

APPENDIX

Degassing of water and carbon dioxide from basaltic magmas can be described using three independent equations (linear and non-linear) describing mass balance, fractionation and speciation of water in the melt. Calculations of degassing paths can be simplified by expressing these equations in terms of three coupled linear differential equations and solving using standard methods of matrix algebra. This approach is described in this Appendix and was developed to describe D/H fractionation during degassing of water from silicate melts (G. Miller & P. Dobson, personal communication, 1990). It has the advantages of being linear and allowing solution of both open and closed system degassing problems with the same equations.

Definition of variables

OH^m	Concentration of water dissolved as hydroxyl groups in the melt (wt %)
H_2O, mol^m	Concentration of water dissolved as molecular water in the melt (wt %)
Total H_2O^m	Total concentration of water in the melt (wt %); Total H_2O (wt %) = OH (wt %) + H_2O mol (wt %)
Total $H_2O^{m,o}$	Initial total concentration water in the melt (wt %)
CO_2^m	Concentration of carbon dioxide dissolved as carbonate in the melt (wt %) (note that though carbon dissolves as carbonate ions in mafic magmas, its concentration is expressed in terms of the weight of CO_2 that dissolves into the melt)
$CO_2^{m,o}$	Initial concentration of carbon dioxide dissolved as carbonate in the melt (wt %)
$N^{m,o}_{\text{Total } H_2O}$	Initial total number of moles of water in the melt; $N^{m,o}_{\text{Total } H_2O}$ = Total $H_2O^{m,o}$/18·015
$N^{m}_{\text{Total } H_2O}$	Total number of moles of water in the melt; $N^{m,o}_{\text{Total } H_2O}$ = Total H_2O^{m}/18·015
N^m_{OH}	Number of moles of OH in the melt; N^m_{OH} = 2(OH^m/18·015)
$N^m_{H_2O,mol}$	Number of moles of molecular water in the melt; $N^m_{\text{Total } H_2O}$ = H_2O, mol/18·015
$N^{m,o}_{CO_3^{2-}}$	Initial number of moles of carbon dioxide dissolved as carbonate in the melt; $N^{m,o}_{CO_3^{2-}}$ = $CO_2^{m,o}$/44·01
$N^m_{CO_3^{2-}}$	Number of moles of carbon dioxide dissolved as carbonate in the melt; $N^m_{CO_3^{2-}}$ = CO_2^m/44·01
$N^v_{H_2O}$	Number of moles of H_2O in the vapor
$N^v_{CO_2}$	Number of moles of CO_2 in the vapor
X_i^m	Mole fraction of species i in melt (single oxygen basis for the silicate component); $X_i^m = [N_i^m/(N^m_{\text{Total } H_2O} + N^m_{CO_3^{2-}} + N^m_O)]$, where N^m_O = (100 − Total H_2O^m − CO_2^m)/36·594
X_i^v	Mole fraction of species i in vapor
a_i^m	Activity of species i in melt
$a_i^{o,m}$	Activity of species i in melt in equilibrium with vapor phase of pure i
f_i	Fugacity of i in the vapor
f_i^o	Fugacity of pure vapor i
$V_i^{o,m}$	Volume of i in the melt in its standard state (cm^3/mol)
f	Fraction of total volatiles remaining in melt; equation (A3)
β	CO_2/H_2O fractionation factor between vapor and melt; equation (A7)
λ	Discriminates between open ($\lambda = 0$) and closed ($\lambda = 1$) system degassing
y	Fraction of H_2O present as OH; equation (A17)
R	Gas constant (83·146 bar cm^3/mol K)
P	Pressure (bars)

Governing equations

Mass balance

The equation of mass balance is defined in terms of f, the fraction of initial water and carbon dioxide remaining in the melt:

$$f = \frac{N^m_{\text{Total } H_2O} + N^m_{CO_3^{2-}}}{N^{m,o}_{\text{Total } H_2O} + N^{m,o}_{CO_3^{2-}}} \tag{A1}$$

Water dissolved in a basaltic melt can exist as hydroxyl groups or as discrete molecules of water. When water enters the melt as hydroxyl groups, one molecule of H_2O reacts with a bridging oxygen to produce two hydroxyl groups; therefore, the H_2O mass balance equation is

$$N^m_{\text{Total } H_2O} = 0{\cdot}5N^m_{OH} + N^m_{H_2O,mol}. \tag{A2}$$

Substitution of equation (A2) into (A1) gives

$$f = \frac{0{\cdot}5N^m_{OH} + N^m_{H_2O,mol} + N^m_{CO_3^{2-}}}{N^{m,o}_{\text{Total } H_2O} + N^{m,o}_{CO_3^{2-}}}. \tag{A3}$$

Differentiating equation (A3) with respect to f gives

$$\frac{0{\cdot}5dN^m_{OH}}{df} + \frac{-dN^m_{H_2O,mol}}{df} = \frac{dN^m_{CO_3^{2-}}}{df} = N^{m,o}_{\text{Total } H_2O} + N^{m,o}_{CO_3^{2-}}. \tag{A4}$$

In both open and closed system degassing, we can equate the differential gain of water and carbon dioxide in the vapor with the differential loss from the melt:

$$\frac{dN^v_{CO_2}}{df} = -\frac{dN^m_{CO_3^{2-}}}{df} \tag{A5}$$

and

$$\frac{dN^v_{H_2O}}{df} = -\frac{dN^m_{\text{Total } H_2O}}{df} = -\frac{0{\cdot}5dN^m_{OH}}{df} - \frac{dN^m_{H_2O,mol}}{df} \tag{A6}$$

Fractionation

Given accurate descriptions of the solubilities of water and carbon dioxide in basaltic melts, and assuming that the CO_2/H_2O of the exsolving vapor is controlled by their relative solubilities and not by kinetic effects, we can express this equilibrium partitioning of water and carbon dioxide into the vapor phase in terms of a single ratio of $\beta_{CO_2\text{-}H_2O,mol}$:

$$\beta_{CO_2-H_2O,mol} = \left(\frac{N^v_{CO_2}}{N^v_{H_2O}}\right) \Big/ \left(\frac{N^m_{CO_3^{2-}}}{N^m_{H_2O,mol}}\right). \quad (A7)$$

Solubilities are expressed in terms of fugacities and mole fractions of components in the melt; therefore, we need to express β in terms of these variables. Because the denominators cancel, the ratio of the number of moles is the same as the ratio of the mole fractions of H_2O and CO_2. For the fugacities of H_2O and CO_2 in the vapor phase, we can greatly simplify the calculation by assuming ideal mixing between H_2O and CO_2 in the vapor (the Lewis–Randall rule):

$$f_i = X^v_i f^\circ_i. \quad (A8)$$

Fugacities of H_2O and CO_2 in H_2O–CO_2 mixtures calculated using the Lewis–Randall rule tend to be higher than those calculated using the modified Redlich–Kwong equation of state for H_2O–CO_2 mixtures (Holloway, 1977). By definition, the fugacities calculated by the two different methods are the same in the limit of pure H_2O or pure CO_2 vapor. For an individual species, the discrepancy between the two fugacity calculations increases as the proportion of that species in the vapor decreases. For the purposes of these calculations, when the proportion of an individual species in the vapor is small, the concentration of that species dissolved in the melt is also relatively small, so the error resulting from the use of the Lewis–Randall rule is focused on the minor component (large relative error–small absolute error). In addition, the maximum discrepancy between the two calculations (when the proportion of a given species in the vapor is small) increases with increasing pressure. At 100 bar pressure, the maximum discrepancy is ~2%, whereas at 1000 bar pressure, this discrepancy is as much as 20%.

The ratio of the number of moles of CO_2 and H_2O in the vapor can now be expressed in terms of fugacities by

$$\left(\frac{N^v_{CO_2}}{N^v_{H_2O}}\right) = \left(\frac{X^v_{CO_2}}{X^v_{H_2O}}\right) = \left(\frac{f_{CO_2}/f^\circ_{CO_2}}{f_{H_2O}/f^\circ_{H_2O}}\right). \quad (A9)$$

We can now define β as

$$\beta_{CO_2-H_2O,mol} = \left(\frac{f^\circ_{H_2O}}{f^\circ_{CO_2}}\right)\left[\left(\frac{f_{CO_2}}{f_{H_2O}}\right) \Big/ \left(\frac{X^m_{CO_3^{2-}}}{X^m_{H_2O,mol}}\right)\right]. \quad (A10)$$

The value of β will be a function of pressure. The pressure dependences of the mole fractions of carbonate and molecular water in basaltic melts at $T = 1200°C$ were determined by Dixon *et al.* (1995) and are given in equations (3) and (4). Substituting equations (3) and (4) into the definition of β gives

$$\beta_{CO_2-H_2O,mol} = 86{\cdot}3\left(\frac{f^\circ_{H_2O}}{f^\circ_{CO_2}}\right)\left[\frac{\exp\{-12(P-1)/[(83{\cdot}15)(1473{\cdot}15)]\}}{\exp\{-23(P-1)/[(83{\cdot}15)(1473{\cdot}15)]\}}\right]. \quad (A11)$$

Differentiating equation (A7) with respect to f, the fraction of initial water and carbon dioxide remaining in the melt, gives

$$\beta N^m_{CO_3^{2-}}\left(\frac{dN^v_{H_2O}}{df}\right) + \beta N^v_{H_2O}\left(\frac{dN^m_{CO_3^{2-}}}{df}\right) - N^v_{CO_2}\left(\frac{dN^m_{H_2O,mol}}{df}\right) - N^m_{H_2O,mol}\left(\frac{dN^v_{CO_2}}{df}\right) = 0. \quad (A12)$$

The vapor phase abundances can be expressed as

$$N^v_{H_2O} = \lambda\left(N^{m,o}_{Total\ H_2O} - 0{\cdot}5N^m_{OH} - N^m_{H_2O,mol}\right) \quad (A13)$$

$$N^v_{CO_2} = \lambda\left(N^{m,o}_{CO_3^{2-}} - N^m_{CO_3^{2-}}\right) \quad (A13)$$

where $\lambda = 1$ for closed system degassing and zero for open system degassing. Combining equations (A12)–(A14) gives

$$-0{\cdot}5\beta N^m_{CO_3^{2-}}\left(\frac{dN^m_{OH}}{df}\right) + \left[(\lambda-\beta)N^m_{CO_3^{2-}} - \lambda N^{m,o}_{CO_3^{2-}}\right]\left(\frac{dN^m_{H_2O,mol}}{df}\right) + \left[\beta\lambda\left(N^{m,o}_{Total\ H_2O} - 0{\cdot}5N^m_{OH} - N^m_{H_2O,mol}\right) + N^m_{H_2O,mol}\right]\left(\frac{dN^m_{CO_3^{2-}}}{df}\right) = 0. \quad (A15)$$

Speciation

The distribution of water between hydroxyl groups and molecular water species in basaltic melt as a function of total water is defined by

$$-\ln\left[\frac{(X^m_{OH})^2}{(X^m_{Total\ H_2O} - 0{\cdot}5X^m_{OH})(1 - X^m_{Total\ H_2O} - 0{\cdot}5X^m_{OH})}\right] = A' + (B' - 0{\cdot}5C')X^m_{OH} + C'X^m_{Total\ H_2O} \quad (A16)$$

where $A' = 0{\cdot}403$, $B' = 15{\cdot}333$ and $C' = 10{\cdot}894$, and $X^m_{H_2O,mol} = X^m_{Total\ H_2O} - 0{\cdot}5X^m_{OH}$ [Dixon *et al.* (1995), using Silver *et al.* (1990) equation (A.5)]. An equivalent equation does not exist for CO_2 because CO_2 dissolves in basaltic melts only as carbonate groups. It is convenient to define a variable, y, as the fraction of total water present as OH groups:

$$y = \frac{0{\cdot}5N^m_{OH}}{0{\cdot}5N^m_{OH} + N^m_{H_2O,mol}} = \frac{N^m_{OH}}{N^m_{OH} + 2N^m_{H_2O,mol}}. \quad (A17)$$

Rearranging and differentiating with respect to f yields

$$(y-1)\frac{dN^m_{OH}}{df} + 2y\frac{dN^m_{H_2O,mol}}{df} = \frac{-dy}{df}(N^m_{OH} + 2N^m_{H_2O,mol}). \quad (A18)$$

This equation contains the term (dy/df), which must be expressed in terms of (dN^m_{OH}/df) or $(dN^m_{H_2O,mol}/df)$. Using the chain rule, (dN^m_{OH}/df) can be expressed as

$$\frac{dN^m_{OH}}{df} = \left(\frac{dN^m_{OH}}{dy}\right)\left(\frac{dy}{df}\right). \quad (A19)$$

Therefore, (dy/df) is equivalent to

$$\frac{dy}{df} = \left(\frac{dN^m_{OH}}{df}\right) \Big/ \left(\frac{dN^m_{OH}}{dy}\right). \quad (A20)$$

An analytical expression for (dN^m_{OH}/dy) is obtained by fitting a sixth-order polynomial through X^m_{OH} vs y data for basalt (Dixon *et al.*, 1995). The fit has an R^2 of 0·999997 and is given by

$$X^m_{OH} = 0{\cdot}00810 + 0{\cdot}68104y - 2{\cdot}72907y^2 + 5{\cdot}92293y^3 - 7{\cdot}67949y^4 + 5{\cdot}36963y^5 - 1{\cdot}57300y^6. \quad (A21)$$

The derivative of equation (A21) with respect to y is

$$\left(\frac{dX^m_{OH}}{dy}\right) = 0{\cdot}68104 + 5{\cdot}45815y + 17{\cdot}76879y^2 - 30{\cdot}71796y^3 + 26{\cdot}84815y^4 - 9{\cdot}43803y^5. \quad (A22)$$

As

$$N^m_{OH} = X^m_{OH}(N^m_{\text{Total } H_2O} + N^m_{CO_3^{2-}} + N^m_O) \quad (A23)$$

then

$$\left(\frac{dN^m_{OH}}{df}\right) = (N^m_{\text{Total } H_2O} + N^m_{CO_3^{2-}} + N^m_O)\left(\frac{dX^m_{OH}}{dy}\right). \quad (A24)$$

Now that (dN^m_{OH}/dy) can be evaluated for each iteration, we can combine equations (A18), (A19) and (A24) to obtain the final differential equation for speciation of water in the melt:

$$\left[(y-1)\left(\frac{dN^m_{OH}}{dy}\right) + N^m_{OH} + 2N^m_{H_2O,mol}\right]\left(\frac{dN^m_{OH}}{df}\right) + 2y\left(\frac{dN^m_{OH}}{dy}\right)\left(\frac{dN^m_{H_2O,mol}}{df}\right) = 0. \quad (A25)$$

Summary of equations describing mass balance, fractionation and speciation

The three final differential equations are:
mass balance:

$$\frac{0{\cdot}5dN^m_{OH}}{df} + \frac{dN^m_{H_2O,mol}}{df} + \frac{dN^m_{CO_3^{2-}}}{df} = N^{m,o}_{\text{Total } H_2O} + N^{m,o}_{CO_3^{2-}} \quad (A4)$$

fractionation:

$$-0{\cdot}5\beta N^m_{CO_3^{2-}}\left(\frac{dN^m_{OH}}{df}\right) + \left[(\lambda-\beta)N^m_{CO_3^{2-}} - \lambda N^{m,o}_{CO_3^{2-}}\right]\left(\frac{dN^m_{H_2O,mol}}{df}\right) + \left[\beta\lambda\left(N^{m,o}_{\text{Total } H_2O} - 0{\cdot}5N^m_{OH} - N^m_{H_2O,mol}\right) + N^m_{H_2O,mol}\right]\left(\frac{dN^m_{CO_3^{2-}}}{df}\right) = 0. \quad (A15)$$

and speciation:

$$\left[(y-1)\left(\frac{dN^m_{OH}}{df}\right) + N^m_{OH} + 2N^m_{H_2O,mol}\right]\left(\frac{dN^m_{OH}}{df}\right) + 2y\left(\frac{dN^m_{OH}}{dy}\right)\left(\frac{dN^m_{H_2O,mol}}{df}\right) = 0. \quad (A25)$$

These equations can be solved simultaneously for the derivatives (dN^m_{OH}/df), $(dN^m_{H_2O,mol}/df)$ and $(dN^m_{CO_3^{2-}}/df)$. These derivatives are calculated by casting equations (A4), (A15), and (A25) into the form of a matrix equation ($\boldsymbol{AX} = \boldsymbol{B}$):

$$\begin{bmatrix} 0{\cdot}5 & 1 & 1 \\ -0{\cdot}5\beta N^m_{CO_3^{2-}} & \left[(\lambda-\beta)N^m_{CO_3^{2-}} - \lambda N^{m,o}_{CO_3^{2-}}\right] & \left[\beta\lambda(N^{m,o}_{\text{Total } H_2O} - 0{\cdot}5N^m_{OH} - N^m_{H_2O,mol}) + N^m_{H_2O,mol}\right] \\ \left[(y-1)\left(\frac{dN^m_{OH}}{dy}\right) + N^m_{OH} + 2N^m_{H_2O,mol}\right] & 2y\left(\frac{dN^m_{OH}}{dy}\right) & 0 \end{bmatrix} \times \begin{bmatrix} \left(\frac{dN^m_{OH}}{df}\right) \\ \left(\frac{dN^m_{H_2O,mol}}{df}\right) \\ \left(\frac{dN^m_{CO_3^{2-}}}{df}\right) \end{bmatrix} = \begin{bmatrix} (N^{m,o}_{\text{Total } H_2O} + N^{m,o}_{CO_3^{2-}}) \\ 0 \\ 0 \end{bmatrix}. \quad (A26)$$

This matrix equation can be solved using standard techniques and the vector of derivatives can be integrated numerically to yield the abundances of hydroxyl groups, molecular water and carbon dioxide in the melt as a function of f, the fraction of initial water and carbon dioxide remaining in the melt.

Discussion of degassing program

A computer program has been written to calculate progressive degassing of a packet of basaltic magma at a given pressure and 1200°C. The calculation begins with a specified pressure, initial water and carbon dioxide contents, and f set to unity. For open system degassing, λ is set to zero (equivalent to setting H_2O^v and CO_2 to zero for each degassing iteration). For closed system degassing, λ is set to unity. The values for $f^o_{H_2O}$, $f^o_{CO_2}$ and β are computed as a function of pressure and are constants at each pressure step.

The program next computes the changes in melt and vapor compositions at constant pressure with progressive degassing of increments of initial volatiles present ($-df$). For each increment the number of moles of hydrous species (N^m_{OH} and $N^m_{H_2O,mol}$) and carbon dioxide ($N^m_{CO_3^{2-}}$), and dy/df are calculated. Substitution of the numeric values of y, dy/df, β, dN^m_{OH}/dy, and the melt species concentrations N^m_{OH}, $N^m_{H_2O,mol}$ and $N^m_{CO_3^{2-}}$ into equation (A26) gives a 3×3 matrix equation for (dN^m_{OH}/df), $(dN^m_{H_2O,mol}/df)$ and $(dN^m_{CO_3^{2-}}/df)$. The values of these derivatives are determined using an LU decomposition solution to the matrix equation (Heilbornn, 1981, p. 76).

For each degassing increment the total dissolved volatile content (H_2O and CO_2) drops by an amount $-df$. The concentrations of the melt species drop by amounts $-df(dN^m_{OH}/df)$, $-df(dN^m_{H_2O,mol}/df)$ and $-df(dN^m_{CO_3^{2-}}/df)$, respectively. The abundances and f are changed by the appropriate amount, and new values of y and dy/df are calculated. The matrix equations are solved again, now using the updated abundances. These steps are repeated until saturation at a given pressure is reached. Saturation is defined by

$$\frac{a^m_{H_2O}}{a^{o,m}_{H_2O}} + \frac{a^m_{CO_3^{2-}}}{a^{o,m}_{CO_3^{2-}}} = \frac{X^m_{H_2O,mol}}{X^{o,m}_{H_2O,mol}} + \frac{X^m_{CO_3^{2-}}}{X^{o,m}_{CO_3^{2-}}} = 1 \quad (A27)$$

where the activities of the species in the melt are the mole fractions of molecular water and carbon dioxide in the melt after each iteration, and the activities of the species in the melt in equilibrium with a pure vapor phase are calculated using equations (3) and (4) in Dixon *et al.* (1995). Degassing paths are modeled by repeating the calculations at progressively lower pressures.

A copy of the program and sample calculations are available on request.